International Geology Review
Publication details, including instructions for authors and subscription information:
http://www.informaworld.com/smpp/title~content=t902953900

Age, geochemical composition, and distribution of Oligocene ignimbrites in the northern Sierra Nevada, California: implications for landscape morphology, elevation, and drainage divide geography of the Nevadaplano

Elizabeth J. Cassel [a]; Andrew T. Calvert [b]; Stephan A. Graham [a]
[a] Department of Geological and Environmental Sciences, Stanford University, Stanford, CA, USA [b] United States Geological Survey, Menlo Park, CA, USA

First Published:July2009

To cite this Article Cassel, Elizabeth J., Calvert, Andrew T. and Graham, Stephan A.(2009)'Age, geochemical composition, and distribution of Oligocene ignimbrites in the northern Sierra Nevada, California: implications for landscape morphology, elevation, and drainage divide geography of the Nevadaplano',International Geology Review,51:7,723 — 742

To link to this Article: DOI: 10.1080/00206810902880370

URL: http://dx.doi.org/10.1080/00206810902880370

International Geology Review
Vol. 51, Nos. 7–8, July–August 2009, 723–742

Age, geochemical composition, and distribution of Oligocene ignimbrites in the northern Sierra Nevada, California: implications for landscape morphology, elevation, and drainage divide geography of the Nevadaplano

Elizabeth J. Cassel[a]*, Andrew T. Calvert[b] and Stephan A. Graham[a]

[a]*Department of Geological and Environmental Sciences, Stanford University, Stanford, CA 94305, USA;* [b]*United States Geological Survey, Menlo Park, CA 94025, USA*

(*Accepted 9 March 2009*)

To gain a better understanding of the topographic and landscape evolution of the Cenozoic Sierra Nevada and Basin and Range, we combine geochemical and isotopic age correlations with palaeoaltimetry data from widely distributed ignimbrites in the northern Sierra Nevada, California. A sequence of Oligocene rhyolitic ignimbrites is preserved across the modern crest of the range and into the western foothills. Using trace and rare earth element geochemical analyses of volcanic glass, these deposits have been correlated to ignimbrites described and isotopically dated in the Walker Lane fault zone and in central Nevada (Henry *et al.*, 2004, Geologic map of the Dogskin mountain quadrangle; Washoe County, Nevada; Faulds *et al.*, 2005, Geology, v. 33, p. 505–508). Ignimbrite deposits were sampled within the northern Sierra Nevada and western Nevada, and four distinct geochemical compositions were identified. The majority of samples from within the northern Sierra Nevada have compositions similar to the tuffs of Axehandle Canyon or Rattlesnake Canyon, both likely sourced from the same caldera complex in either the Clan Alpine Mountains or the Stillwater Range, or to the tuff of Campbell Creek, sourced from the Desatoya Mountains caldera. New $^{40}Ar/^{39}Ar$ age determinations from these samples of 31.2, 30.9, and 28.7 Ma, respectively, support these correlations. Based on an Oligocene palinspastic reconstruction of the region, our results show that ignimbrites travelled over 200 km from their source calderas across what is now the crest of the Sierra Nevada, and that during that time, no drainage divide existed between the ignimbrite source calderas in central Nevada and sample locations 200 km to the west. Palaeoaltimetry data from Sierra Nevada ignimbrites, based on the hydrogen isotopic composition of hydration water in glass, reflect the effect of a steep western slope on precipitation and indicate that the area had elevations similar to the present-day range. These combined results suggest that source calderas were likely located in a region of high elevation to the east of the Oligocene Sierra Nevada, which had a steep western slope that allowed for the large extent and broad distribution of the ignimbrites.

Keywords: Sierra Nevada; palaeotopography; ignimbrites; Oligocene; landscape evolution

Introduction

The tectonic processes that control the development and evolution of mountain belts and orogenic plateaus are reflected in large-scale topographic and geomorphic changes,

*Corresponding author. Email: ecassel@stanford.edu

ISSN 0020-6814 print/ISSN 1938-2839 online

DOI: 10.1080/00206810902880370
http://www.informaworld.com

together with regional climate, and the record of these changes can thus provide information on crustal, lithospheric, and upper mantle dynamics (England and Molnar 1990; Whipple *et al.* 1999; Rowley *et al.* 2001). The Sierra Nevada has been studied for over a century, but questions remain regarding the topographic and geomorphic histories of the range and its pre-extension relationship to the Basin and Range region. Although long thought to be the product of very recent uplift (e.g. Lindgren 1911; Jones *et al.* 2004), some recent studies have proposed that the area now occupied by the Sierra Nevada was uplifted in the Late Cretaceous–early Cenozoic and has remained high throughout the Cenozoic (e.g. Wernicke *et al.* 1996; House *et al.* 2001; Poage and Chamberlain 2001; Mulch *et al.* 2006, 2008; Cassel *et al.* 2009). The area may have been the western edge of a high-elevation plateau – the 'Nevadaplano' that covered much of what is now Nevada and western Utah – similar to the Andean Altiplano (cf. Wolfe *et al.* 1997, 1998; DeCelles 2004). To gain a better understanding of the topographic and landscape evolution of the Sierra Nevada–Basin and Range region and the timing of Sierra Nevada surface uplift, we integrate a regional palaeoaltimetry study with an analysis of landscape morphology based on ignimbrite correlations across the region. This study constrains the timing and amount of changes in topography and geomorphology in the northern Sierra Nevada and western Basin and Range, which have implications for the orogenic processes that drove the evolution of both regions.

We combine geochemical and isotopic age correlations of widely distributed ignimbrites in the northern Sierra Nevada (Figure 1) with recent palaeoaltimetry data to trace the extent of palaeodrainages, quantify the change in elevation over the length of Oligocene drainages, and characterize the Oligocene landscape morphology of the Sierra Nevada and Nevadaplano. We present new trace and rare earth element (TREE) geochemical data and $^{40}Ar/^{39}Ar$ radiometric age determinations (Figures 2 and 3), which we use to correlate Sierra Nevada ignimbrites to informally named tuffs in western and central Nevada, including the tuff of Axehandle Canyon (TAXC), the tuff of Rattlesnake Canyon (TRC) and the tuff of Campbell Creek (TCC; Henry *et al.* 2004). These data show that the regional drainage divide, which now resides west of the California–Nevada border, was located in central–eastern Nevada in the Oligocene, at least 200 km east of its present position, when subsequent Basin and Range extension is removed (Figures 1 and 4). These results, combined with our previous palaeoaltimetry work (Figure 5; Cassel *et al.* 2009), show that the Oligocene Sierra Nevada formed the steep western slope of a region of high topography, possibly an orogenic plateau, where ignimbrite source calderas were located. The ignimbrites, constrained in palaeovalleys (Faulds *et al.* 2005) and aided by this topographic gradient, were able to travel over 200 km from their sources.

Geologic framework

Pre-Cenozoic basement on the western slope of the northern Sierra Nevada consists of an amalgam of Palaeozoic–Mesozoic continental margin and accretionary prism metasedimentary and metavolcanic rock, intruded by Jurassic to Late Cretaceous tonalite and granodiorite emplaced during continental arc magmatism (Chen and Moore 1982; Girty *et al.* 1996; Ducea 2001). The northern part of the range has lower mean and peak elevations than the south; the deepest batholithic rocks are exposed in the south (Ague and Brimhall 1988), whereas Cenozoic cover strata, well preserved in the north, are not generally present in the south.

Fluvial 'auriferous gravel' or 'prevolcanic gravel' (exposed by hydraulic gold mining from 1853–1882) is deposited on basement in the northern Sierra Nevada and is composed of

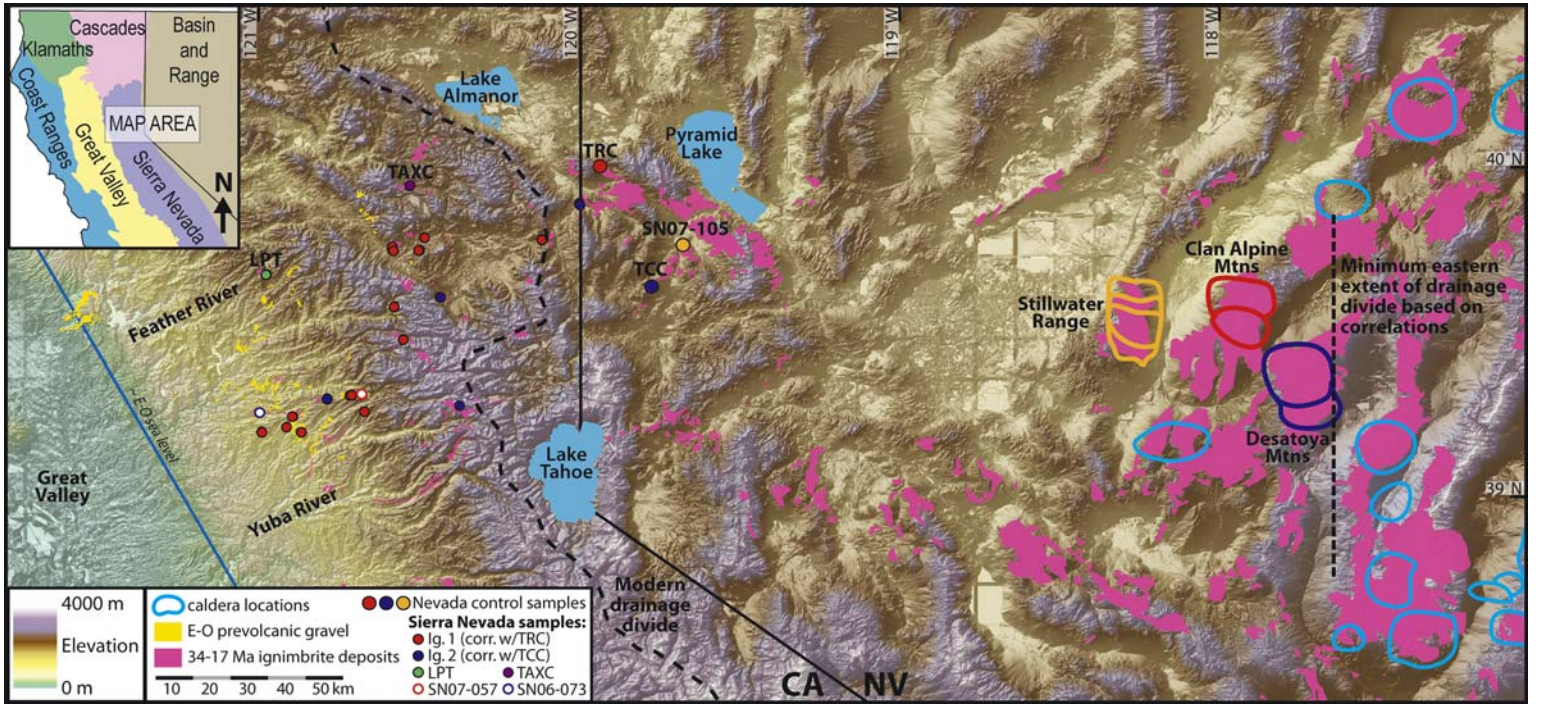

Figure 1. Map of study area and source caldera locations in the northern Sierra Nevada of California and northwestern–central Nevada; inset shows map location and major geologic regions of northern California and Nevada. Oligocene ignimbrite sample localities indicated by points, large points indicate western Nevada control samples, geochemically distinct ignimbrites grouped by colour; red: correlative with the TRC; blue: correlative with the TCC; open red and blue: possible correlative samples; purple: 31.2 Ma sample correlative with the TAXC; yellow: SN07-105 – tuff of Chimney Spring or tuff of Painted Hills; green: La Porte Tuff (LPT). Prevolcanic gravel deposits shown in yellow; mid-Cenozoic ignimbrite deposits shown in pink; drainage divides represented by black dashed lines; likely source calderas for TAXC/TRC, TCC and SN07-105 outlined in red, dark blue, and yellow; other known and inferred Oligocene caldera locations outlined in light blue (from John *et al.* 2008). Digital elevation model from The National Map: US Geological Survey; geology compiled from Saucedo and Wagner (1992), Henry *et al.* (2004) and Crafford (2007) and mapping by Cassel.

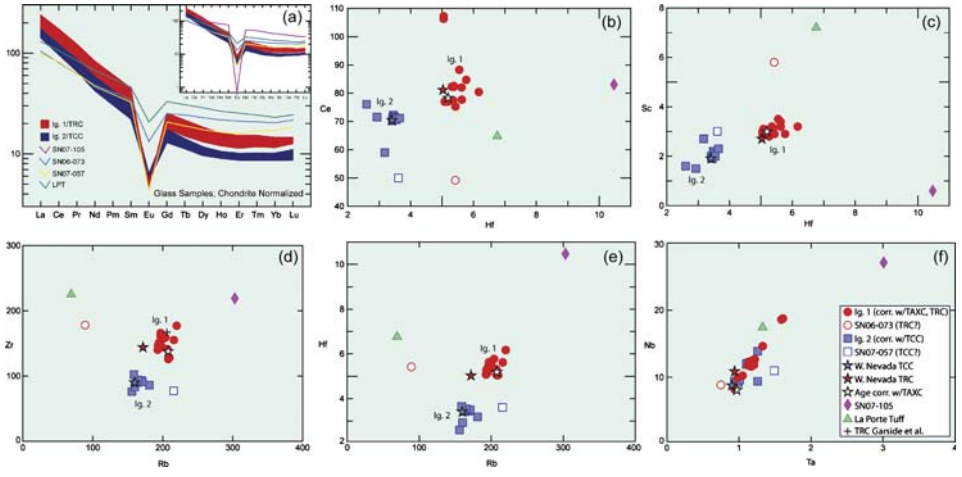

Figure 2. Comparison of TREE compositions of volcanic glass from unwelded zones of ignimbrites from the northern Sierra Nevada and western Basin and Range. (a) Chondrite-normalized TREE patterns show range of sample values, and more evolved character of ignimbrite 1 samples (red) compared with ignimbrite 2 (blue); inset shows all samples including SN07-105 (chondrite values from Sun and McDonough 1989). (b–f) Individual element concentrations (in ppm) for all samples. SN07-105 (purple) spider pattern and element signature indicates a highly evolved, high silica rhyolite ignimbrite, distinct from all other samples (sample from either the tuff of Chimney Spring or tuff of Painted Hills). LPT (green triangle) element signature is the least evolved and likely indicates a different source. SN06-073 (open circle) and SN07-057 (open square) have less evolved compositions, but could correlate to TRC and TCC, respectively.

Eocene–Oligocene gravel, sand, and minor clay (Figure 6; Lindgren 1911; Bateman and Wahrhaftig 1966). Middle–late Eocene flora from within the upper half of the sequence are the only dateable material in the prevolcanic gravel (MacGinitie 1941). When Oligocene volcanic units are present, the top of the prevolcanic gravel is either marked by an erosional unconformity with overlying Oligocene ignimbrite deposits, or Oligocene ignimbrite and volcaniclastic deposits are interbedded with non-volcanic fluvial deposits, showing that aggradation continued in the drainage system from Eocene to Oligocene (Figures 6 and 7).

Oligocene rhyolitic ignimbrite, tuffaceous palaeosol horizons, and volcaniclastic fluvial sand, generally referred to as either the Delleker (Northern Sierra) or Valley

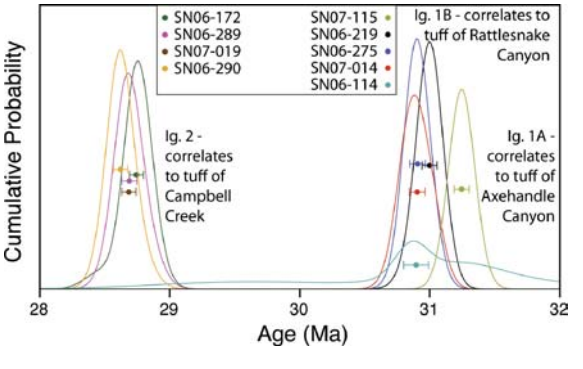

Figure 3. Cumulative probability plot of all $^{40}Ar/^{39}Ar$ radiometric ages from nine of the 10 analysed samples. Weighted means and errors (2σ) are plotted for each sample. See supplementary material online at www.informaworld.com/tigr for individual age determinations and analytical techniques.

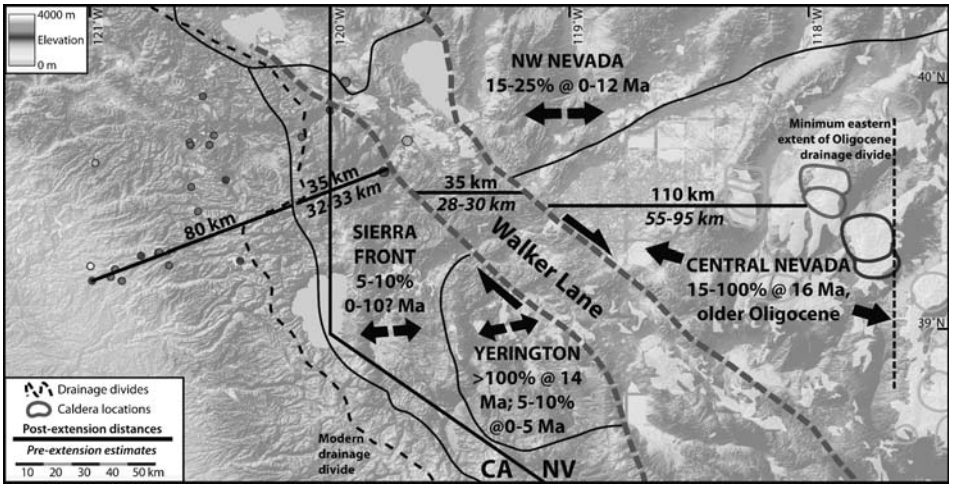

Figure 4. Map showing distance travelled by ignimbrites, divided by Basin and Range extensional and dextral shear domains. Distance travelled after removing extension in italics, based on estimates as shown. Ignimbrites directly travelled approximately 200–240 km. Extension mapping modified from Van Buer *et al.* (2009); estimates from Seedorf (1991); Smith *et al.* (1991); Surpless *et al.* (2002); Faulds *et al.* (2005) and Colgan *et al.* (2006).

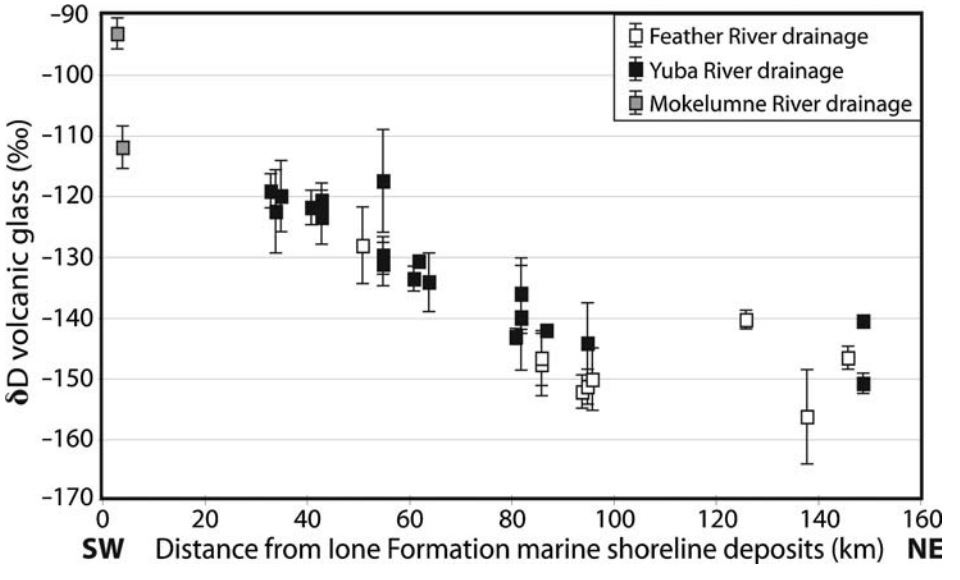

Figure 5. Stable isotope palaeoaltimetry results from Cassel *et al.* (2009): hydrogen isotopic composition of hydration water from volcanic glass (δD‰) versus distance of sample from Ione formation marine shoreline deposits (eastern edge of the Great Valley). Glass sampled from ignimbrites at modern elevations ranging from 200 to 1920 m. Black: Yuba River drainage samples; white: Feather River drainage samples; grey: Mokelumne River drainage samples. Values represent averages of three to nine analyses of each sample, 2σ error bars.

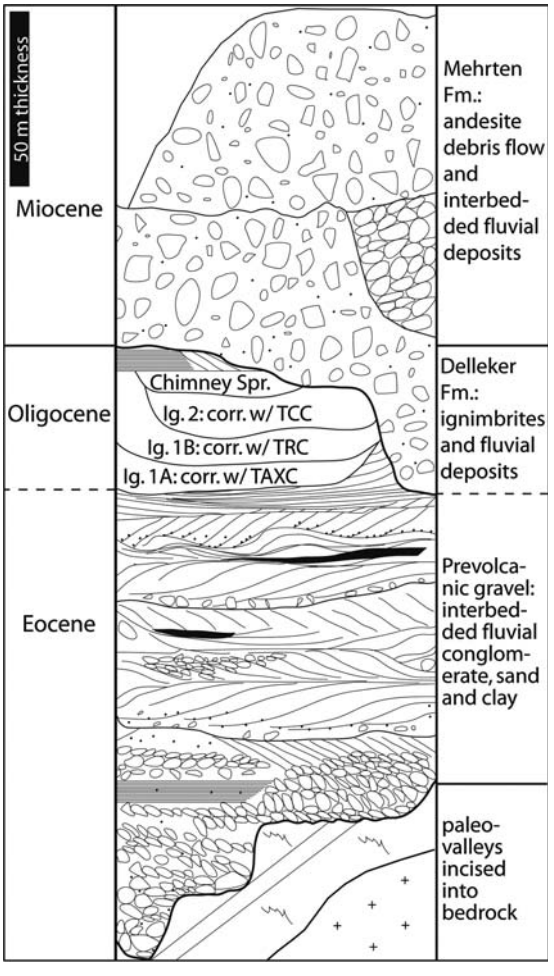

Figure 6. Generalized Cenozoic stratigraphy in the northern Sierra Nevada; unit thicknesses approximated for 1000 m present-day elevation. Age references cited in text.

Springs (Central Sierra) formations (Dalrymple 1964; Wagner *et al.* 2000), overlie the prevolcanic gravel or lie in buttressed unconformity on the basement (Figure 6). K/Ar and $^{40}Ar/^{39}Ar$ ages on these formations range from 20.5 to 33.4 Ma in the northern Sierra Nevada (Dalrymple 1964; Evernden and James 1964; Deino 1985, 1989; Saucedo *et al.* 1992; Wolfe 1992; Brooks *et al.* 2008). Early work on these units suggested that both formations were the products of an early period of rhyolitic volcanism in the Sierra Nevada prior to the eruption of Miocene andesitic volcanic units (Mehrten formation) (cf. Durrell 1959; Dalrymple 1964), but recent studies have proposed that these ignimbrites may have been sourced from further east in Nevada (e.g. Brooks *et al.* 2003, 2008; Faulds *et al.* 2005; Garside *et al.* 2005).

Cenozoic magmatism began in northeastern Nevada at about 45 Ma, as part of a southward migrating sweep of magmatism, culminating in the Oligocene 'ignimbrite flare-up' in central Nevada, which resulted in the production of approximately 50,000 km^3 of rhyolitic and dacitic ignimbrites from an estimated 50 calderas (Best *et al.* 1989; Best and Christiansen 1991; Henry 2008). Faulds *et al.* (2005) recognized 16

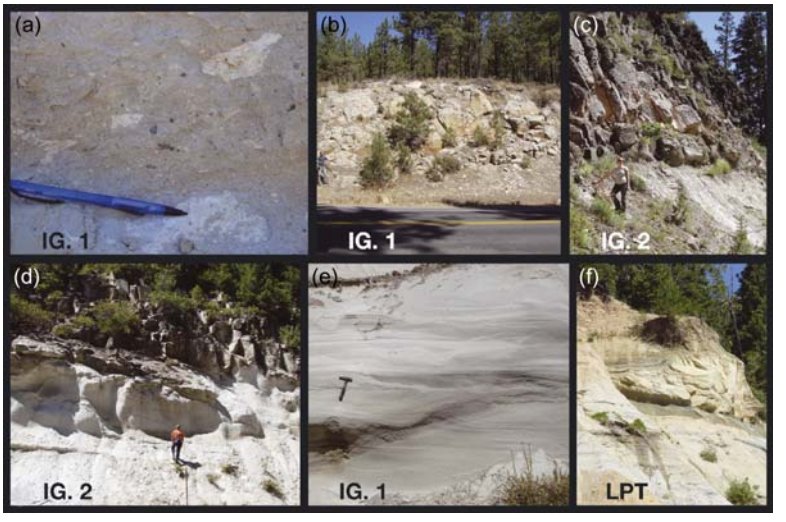

Figure 7. Photos of Sierra Nevada ignimbrite deposits: (a) Detail of pumice and lithics in ignimbrite 1; (b) Exposure of ignimbrite 1 at Delleker, correlative to TRC; (c) ignimbrite 2 at Soda Springs, correlative with TCC; (d) ignimbrite 2 along Hwy 20, correlative with TCC; (e) reworked ash and fluvial deposits at You Bet/Chalk Bluff, overlying ignimbrite 1; (f) LPT interbedded with fluvial sediments.

distinct Oligocene ignimbrites (ranging from 32 to 24 Ma), erupted from calderas in central Nevada, interbedded with sedimentary strata in palaeovalleys extending from western Nevada west across the northern Walker Lane fault system, and correlated them based on mapping, petrography, and $^{40}Ar/^{39}Ar$ dating. In western Nevada, the ignimbrite sequence ranges in thickness from 200 to 700 m, and ignimbrites are often interbedded with volcaniclastic fluvial sediments. The sequence described by Faulds *et al.* (2005) includes the following ignimbrites (Figure 1): the TAXC (31.2 ± 0.1 Ma; Brooks *et al.* 2008) and the TRC (31.0 ± 0.1 Ma), both likely sourced from the Clan Alpine Mountains or the Stillwater Range; the TCC (28.8 ± 0.1 Ma), sourced from the Desatoya Mountains caldera; and the tuff of Chimney Spring (25.1 ± 0.1 Ma) and the tuff of Painted Hills (24.9 ± 0.1 Ma), both likely erupted from calderas in the Stillwater Range (John 1995). These ignimbrites were sampled in western Nevada as possible correlative units to Sierra Nevada ignimbrites, based on field occurrence and petrographic similarities.

Brooks *et al.* (2003) identified a sequence of nine ignimbrite units (Tuffs A–I) and interbedded conglomerates as Delleker formation, exposed at Haskell Peak, CA, within the southern Walker Lane fault zone. They used phenocryst volumes and whole-rock Nb–Rb–Sr–Zr data to correlate the youngest units (G–I) with the Nine Hill Tuff (Deino 1985, 1989) and the tuff of Chimney Spring. With the addition of $^{40}Ar/^{39}Ar$ sanidine single-crystal ages, Brooks *et al.* (2008) correlated the older units (A, B, and F) with the TAXC, TRC and TCC, respectively. They also suggest that the character of incision, morphology of the ignimbrites, and sequence of units and unconformities at Haskell Peak define a west-sloping Eocene–Oligocene palaeovalley. No widespread geochemical fingerprinting and isotopic dating has been conducted prior to this study to establish unit-specific correlations or quantify the full spatial extent of ignimbrites throughout the northern Sierra Nevada.

Previous research

Many previous studies have suggested that the early Cenozoic Sierra Nevada–Basin and Range region may have formed a high-topography plateau similar to the modern Andes (Molnar and Chen 1983; Coney and Harms 1984; Sonder *et al.* 1987; Wernicke *et al.* 1996; Jones *et al.* 1998; Sonder and Jones 1999; DeCelles 2004). Palaeobotanical data from Nevada support these comparisons, providing estimates of 2–3 km of elevation for the early–middle Cenozoic (Gregory-Wodzicki 1997; Wolfe *et al.* 1997, 1998). Other studies from within the Sierra Nevada, however, propose a low-relief, low-elevation (< 1 km) landscape after Late Cretaceous–early Cenozoic denudation of the volcanic arc (Lindgren 1911; Hudson 1960; Huber 1981, 1990; Unruh 1991; Dilek and Moores 1999; Wakabayashi and Sawyer 2001; Jones *et al.* 2004). Using comparisons between palaeovalley and modern topographic gradients, and projections of progressively tilted strata, these studies propose that the range was then tilted to the southwest as a rigid block between 8.4 and 3.4 Ma, causing between 1500 and 2500 m of uplift at the range crest. Jones *et al.* (2004) suggested the removal of dense lithosphere as a driver for uplift of the range, and this mechanism has also been proposed specifically for the uplift of the southern Sierra (Ducea and Saleeby 1996, 1998; Boyd *et al.* 2004; Zandt *et al.* 2004). The method of projecting the gradient or tilt of Cenozoic sedimentary units, however, relies on uncertain correlation of units with geographically limited exposures. Using this method with the Eocene prevolcanic gravel requires the assumption that synchronous deposition occurred within a connected channel headed near the modern crest of the range (cf. Lindgren 1911). In addition, differences between palaeovalley and modern gradients, and angles of tilted strata, do not necessarily reflect surface movement (cf. England and Molnar 1990; Small and Anderson 1995).

A growing body of evidence from stable isotope palaeoaltimetry, thermochronology, crustal structure, and palaeobotanical studies indicates high topography in what is now the Sierra Nevada throughout the Cenozoic, allowing for little to no late Cenozoic surface uplift (Wolfe *et al.* 1997, 1998; Chamberlain and Poage 2000; Poage and Chamberlain 2002; Horton *et al.* 2004; Cecil *et al.* 2006; Mulch *et al.* 2006, 2008; Crowley *et al.* 2008; Cassel *et al.* 2009). Recent stable isotope palaeoaltimetry studies on the western side of the northern Sierra Nevada show that the range had a steep western gradient, similar to the modern range, in the Eocene and Oligocene (Mulch *et al.* 2006; Cassel *et al.* 2009), and multiple studies also argue for the existence of a Sierra Nevada rain shadow since middle Miocene (cf. Poage and Chamberlain 2002; Horton *et al.* 2004; Crowley *et al.* 2008; Mulch *et al.* 2008). These isotopic studies supply information on the effect of the mean elevation of the orographic barrier on precipitation and climate, but do not fully characterize the landscape within or behind the mountain range. Small elevation changes (< 800 m) and local landscape features in areas behind the orographic barrier, such as the location of the drainage divide, can be obscured by additional moisture sources not controlled by elevation (common on high-elevation plateaus, cf. Tian *et al.* 2007) and are difficult to obtain within the error of the method.

Crustal structure modelling and thermochronology from the southern Sierra Nevada also support Cenozoic high topography (Wernicke *et al.* 1996; House *et al.* 1997, 1998, 2001). Based on xenolith, seismic, and crustal strain data, Wernicke *et al.* (1996) found that crust in the southern Sierra Nevada is similar in thickness to that in the highly extended Basin and Range, and suggested that the area maintained high or slightly decreasing elevations through the Cenozoic. Using (U–Th)/He ages, House *et al.* (1998, 2001) based estimates of palaeoelevation on a systematic variation in palaeotemperature

in the Cretaceous and concluded that ancient fluvial relief and mean elevation in the southern Sierra Nevada have either not changed or gradually lowered in the Cenozoic. Thermochronology along the Yuba River in the northern Sierra Nevada (Cecil *et al.* 2006) showed that total exhumation in the past 60 Ma was < 3 km, with faster exhumation rates in the Cretaceous. These data, however, do not provide the resolution necessary to deduce smaller elevation changes within the Cenozoic (see Farley 2002), and surface uplift cannot be uniquely inferred from thermochronologic methods alone (Small and Anderson 1995).

Multiple studies have suggested that the location of the regional drainage divide shifted significantly to the west in the late Cenozoic (Yeend 1974; Dilek and Moores 1999; Henry 2008). Reconstructing the geomorphology of Oligocene palaeovalleys in the Sierra Nevada, including the lengths of the drainages, the location of the divide or crest, and the amount of valley relief, can aid our interpretations of palaeoelevation gained along the length of these drainages and the amount, if any, of late Cenozoic surface uplift in the range. We use geochemical data and isotopic ages from widely distributed ignimbrites in the northern Sierra Nevada to correlate ignimbrite deposits on both sides of the modern crest. Combined with our palaeoaltimetry data, this enables us to trace the extent of palaeodrainages, quantify the change in elevation over the length of Oligocene drainages, and characterize the Oligocene landscape morphology of the Sierra Nevada and Nevadaplano.

Ignimbrite occurrence and field description

Rhyolitic ignimbrites are widespread throughout the northern Sierra Nevada, preserved under Miocene volcanic and volcaniclastic strata (Figure 1). Three distinct ignimbrite units can be identified based on field and petrographic observations: ignimbrites 1 (A and B) and 2 (Figure 6). Ignimbrites 1A and 1B have been grouped together based on their petrographic and geochemical similarities, suggesting that they are from the same source caldera, but they have distinctive ages, sanidine K/Ca ratios, and phenocryst assemblages (see following sections). All ignimbrite units are vitric, massive to crudely stratified, poorly sorted, and typically contain lithic fragments, glassy white pumice, and over 50% ash (Figure 7). The degree of welding varies between zones and across the Sierra Nevada, from densely to poorly welded near the crest (Brooks *et al.* 2008) to completely unwelded to the west. Pumice clasts typically decrease in maximum size from east to west, ranging from 15 to 2 cm in length. Ignimbrite 1A ranges in colour from dark to light grey, with varying proportions of plagioclase, sanidine, biotite, and rare quartz phenocrysts. In some locations, ignimbrite 1B can be distinguished from 1A because it is relatively crystal-poor and has less biotite and more sanidine. Based on this distinction, it appears that ignimbrite 1B is more widespread throughout the Sierra Nevada, but reworking of low-elevation samples makes differentiating these units difficult. Ignimbrite 2 can be distinguished from ignimbrites 1A and 1B by an overall crystal-poor nature, but with a high proportion of quartz phenocrysts, described as pink to smoky-grey vermiform crystals by Brooks *et al.* (2008). The descriptions and $^{40}Ar/^{39}Ar$ dating in Brooks *et al.* (2008) (Tuffs A, B, F) and the geochemistry and $^{40}Ar/^{39}Ar$ dating presented here support these divisions.

Ignimbrite units are laterally discontinuous and confined to palaeovalleys throughout the Sierra Nevada, indicating significant Oligocene valley relief. Ignimbrites are found both conformably overlying prevolcanic gravel deposits and unconformably deposited over prevolcanic gravel or the basement, and often ignimbrites are interbedded with fluvial deposits (Figures 6 and 7; Brooks *et al.* 2008). In the high Sierra Nevada, one or

more rhyolitic ignimbrite units comprise 50–400 m thick sections. At Haskell Peak, Brooks *et al.* (2008) reported individual units lower in the sequence (Tuffs A–E) varying in thickness from 0 to 75 m, with interbedded conglomerate units no greater than 12 m in thickness, and one ignimbrite (Tuff F) up to 120 m thick northeast of the peak. In the western foothills of the Sierra Nevada, individual unwelded units thin to 20 m or less, and in some areas ignimbrites show evidence of reworking and are capped by Oligocene tuffaceous fluvial deposits and palaeosol horizons (Figure 7). The transition to thinner units is abrupt, and correlates with an increase in frequency, spatial extent, and overall thickness of prevolcanic gravel exposures. This transition is likely a result of widening palaeovalleys and loss of confinement, as underlying fluvial gravels show evidence of braided stream deposition.

In western Nevada, Henry *et al.* (2004) described the TAXC as pink to light brown to grey, pumiceous, and sparsely porphyritic with abundant sanidine, plagioclase, and some biotite. The TAXC is the oldest ignimbrite exposed in the western Nevada sequence described by Faulds *et al.* (2005). The TRC is light red, densely to poorly welded, pumiceous, porphyritic and characterized by abundant sanidine. The TCC typically ranges in colour from dark to light grey to cream, and is sparsely porphyritic with common smoky, vermicular quartz, and plagioclase (Henry *et al.* 2004).

Geochemical correlations

Pure unaltered volcanic glass was isolated from unwelded ignimbrite samples, and analysed for TREE compositions on ICP-MS (Figure 2; see supplementary material for complete results). Glass fractions of 99% purity were prepared through size, magnetic, and gravity separations, and checked for purity and alteration with a petrographic microscope. Samples with any clay alteration or visible birefringence were not analysed. To avoid contamination and hydration issues highlighted by Hildreth and Mahood (1985), we have focused our data analysis and interpretations on the glass chemistry only. Sierra Nevada ignimbrite samples were broken into two populations based on geochemical composition: ignimbrites 1 (A and B) and 2 (Figure 2), and were compared with three samples from western Nevada ignimbrites that were described and mapped by Henry *et al.* (2004) and Garside *et al.* (2003) (Figure 1).

Samples from northern Sierra Nevada ignimbrites and from the TRC and TCC in western Nevada are distinct from sample SN07-105, a highly evolved high-silica rhyolite (Figure 2(a)). Samples from ignimbrite 1 are correlative with the TRC sample, and are widespread throughout the Sierra Nevada (Figure 1), including the type locality of the Delleker formation. Samples from this ignimbrite appear more evolved overall, as shown in the TREE patterns (Figure 2(a)), and have distinctly higher Hf and Rb values, as well as slightly enriched Ce and Sc values, than samples from ignimbrite 2 (Figure 2(b,c)). Because Hf and Sc are highly immobile elements, it is unlikely that these differences are the result of fractionation or weathering processes (Hildreth and Mahood 1985). Samples from ignimbrite 1 are also geochemically similar to a TRC whole-rock sample analysed by Garside *et al.* (2003) (cross: Figure 2(d)). One sample (white star: Figure 2) that yielded a slightly older $^{40}Ar/^{39}Ar$ age (see following section) is geochemically similar to all other ignimbrite 1 samples, suggesting that ignimbrite 1 consists of two units that came from the same source caldera complex. Samples from ignimbrite 2, including a sample taken from Tuff F of Brooks *et al.* (2003, 2008) at Haskell Peak, are correlative with the TCC sample from western Nevada. Zr values for ignimbrite 2 are all near 100 ppm, which is typical for rhyolites and distinctly lower than those of ignimbrite 1 (Figure 2(d)).

Sample SN07-057 (open square, Figure 2) has similar Hf, Ta, Cs, Sc, Zr, and Nb concentrations to ignimbrite 2 and the TCC, but it has lower Ce and higher Rb, indicating it could be a distinct unit. Both Ce and Rb are geochemically mobile, however, and leaching or fractionation could have affected sample concentrations after deposition (Figure 2(b)). In comparison with ignimbrite 2, the flattened, rounded TREE pattern, with a lower Eu anomaly, of sample SN07-057 could be produced by fractionation of the TCC (Figure 2(a)). Based on the similarity of concentrations in most immobile elements and the TREE pattern, it is possible that sample SN07-057 is correlative with ignimbrite 2 and the TCC.

Sample SN06-073 (open circle, Figure 2) has similar Hf, Nb, and Zr values to ignimbrite 1, but it has lower Rb, Ce, Cs, and Ta. Because Ce, Rb, and Cs are more mobile, the pattern shown in Figure 2(b) could be produced by fractionation of the same unit. The TREE pattern of SN06-073 is enriched in both Eu and the heavy rare earth elements in comparison with ignimbrite 1, however, which would not be expected from fractionation (Figure 2(a)). Some elemental concentrations in sample 06-073 are similar to ignimbrite 1, but the TREE pattern appears distinct, and it is possibly from a different unit. Unfortunately, the unit was significantly reworked, and did not yield any grains adequate for $^{40}Ar/^{39}Ar$ dating.

A sample of the La Porte Tuff (LPT) does not appear to correlate with any of the other units sampled in the Sierra Nevada or western Nevada (Figure 2). Wolfe (1992) obtained K/Ar ages for the LPT of 33.1 and 33.3 Ma. The LPT sample is enriched in the heavy rare earth elements, has a relatively high Eu anomaly, and is depleted in Rb and Cs, compared with all other units sampled. This less evolved, more mafic composition may indicate that the tuff was part of an earlier phase of 'ignimbrite flare-up' volcanism. The LPT is a significantly reworked, well-sorted, extremely crystal-poor, water-lain deposit (Figure 7), and based on the immobile element concentrations and TREE pattern, it is likely sourced from an ash fall deposit not within the western Nevada sequence of Faulds *et al.* (2005).

$^{40}Ar/^{39}Ar$ geochronology

Ten new $^{40}Ar/^{39}Ar$ radiometric ages of sanidine and plagioclase phenocrysts were determined to evaluate the geochemical correlations discussed above (Figure 3 and Table 1). Feldspar grains were separated and purified from whole-rock samples using magnetic, hydrofluoric acid (HF) acid etching, and visual separation techniques. Samples were irradiated for 16 h in the central thimble of the US Geological Survey TRIGA reactor using Taylor Creek Sanidine (TCR-2) as an irradiation flux monitor. A total of 132 single-crystal laser-fusion analyses were performed at the US Geological Survey in Menlo Park, CA using a 30W CO_2 laser and analysed on an MAP 216 spectrometer. The standard (TCR-2) age used during analysis was 27.87 Ma; however, all results reported here were recalculated using $R^{TCR-2}_{FCT-2} = 1.006552 \pm 0.000585$ to make them equivalent to a 28.02 Ma Fish Canyon sanidine age to facilitate comparison with results in Henry *et al.* (2004) and Faulds *et al.* (2005). The $^{40}Ar/^{39}Ar$ age determinations are reported with 2σ analytical uncertainties (Figure 3; Table 1). Full analytical techniques, plots, and tabulated data are presented in the supplementary material.

Analyses of 10 samples resulted in four discrete ages that correlate with dated ignimbrite units in western Nevada. Results for three of the four groups appear in Figure 3; the youngest ignimbrite is omitted to better illustrate the older ignimbrites, but is plotted in the supplementary material. Several samples yielded little sanidine and the analysis of

Table 1. All $^{40}Ar/^{39}Ar$ age determinations for sanidine and plagioclase, with locations, number of grains analysed, weighted mean ages, and 2σ errors. MSWD after York (1969).

Sample no.	Latitude	Longitude	Sanidine wt. mean (Ma) (*n*)	Plagioclase wt. mean (Ma) (*n*)	Pooled weighted mean (Ma)	MSWD
SN07-115POA	39.9663667	120.537567	31.24 ± 0.06 (12)	– (0)	31.24 ± 0.06	0.32
SN06-219	39.4963	120.558033	31.01 ± 0.06 (12)	30.93 ± 0.27 (3)	31.00 ± 0.06	0.28
SN06-275	39.5964833	120.586817	30.91 ± 0.06 (12)	30.91 ± 0.26 (3)	30.91 ± 0.06	0.26
SN07-014PO	39.77	120.505767	30.92 ± 0.06 (10)	30.84 ± 0.17 (4)	30.90 ± 0.06	0.76
SN06-114	39.2150167	120.881683	30.85 ± 0.13 (2)	31.09 ± 0.66 (4)	30.89 ± 0.21	1.36
SN06-172	39.29425	120.381617	28.73 ± 0.07 (6)	28.76 ± 0.08 (9)	28.74 ± 0.05	0.66
SN06-289	39.9115667	120.001583	28.67 ± 0.21 (3)	28.70 ± 0.07 (11)	28.69 ± 0.06	0.35
SN07-019RE	39.6623167	119.7768	28.67 ± 0.21 (3)	28.68 ± 0.07 (11)	28.68 ± 0.05	0.72
SN06-290	39.9115667	120.001583	28.62 ± 0.21 (3)	28.62 ± 0.08 (10)	28.62 ± 0.05	0.32
SN07-105RE	39.7859667	119.6739	25.01 ± 0.04 (14)	– (0)	25.01 ± 0.04	0.51

plagioclase improved precision and helped with tuff correlations (Table 1). In all cases, sanidine and plagioclase grains from the ignimbrites yielded results within analytical error, so their pooled weighted means (Table 1) are interpreted as eruption ages. Because none of the 10 samples is from the same location, we do not consider a weighted mean of the discrete groups to be appropriate. Sample SN07-115 yielded 12 concordant analyses with a weighted mean of 31.24 ± 0.06 Ma, and is within error of previous TAXC results (31.2 ± 0.1 Ma; Henry *et al.* 2004; Faulds *et al.* 2005). Additionally, sanidine K/Ca ratios derived from $^{39}Ar/^{37}Ar$ measurements distinguish SN07-115 from other units (supplementary material). Four samples are grouped near 30.9 Ma and likely represent a single unit. SN06-219, SN06-275, SN07-014, and SN06-114 yield overlapping age distributions (Figure 3). The weighted mean age for SN06-219 of 31.00 ± 0.06 Ma only slightly overlaps the identical SN06-275 and SN07-014, but they are chemically similar and erupted at most 100 ka apart. SN06-114 only yielded two sanidine and four plagioclase crystals, so the precision is poor, but the weighted mean matches those of SN06-219 and SN06-275. Considering their geochemical and age similarity, these units all likely correlate with the TRC (31.0 ± 0.1 Ma; Faulds *et al.* 2005). Crystals from four samples (SN06-289, SN07-019, SN06-290, and SN07-105) yielded concordant analyses at 28.7 Ma and correlate well with the TCC (28.8 ± 0.1 Ma; Faulds *et al.* 2005). Sample SN07-105 yielded concordant results of 25.01 ± 0.04 Ma. This sample is likely from the tuff of Chimney Spring (25.1 ± 0.1 Ma; Faulds *et al.* 2005) or the tuff of Painted Hills (24.9 ± 0.1 Ma). K/Ca ratios derived from $^{39}Ar/^{37}Ar$ measurements of SN07-105 are similar to measurements from Faulds *et al.* (2005) of these tuffs as well.

These ages support the correlations made based on the TREE geochemical analyses. Sierra Nevada ignimbrite 1A (sample SN07-115) is correlative with the TAXC in western Nevada (Faulds *et al.* 2005) and with Tuff A of Brooks *et al.* (2008). Samples from ignimbrite 1B are correlative with the TRC in western Nevada (Faulds *et al.* 2005) and with Tuff B of Brooks *et al.* (2008), although age dating may be necessary in crystal-poor samples to distinguish it from ignimbrite 1A, to which it is geochemically similar. The geochemical and petrographic similarities of ignimbrites 1A and 1B, and their difference in eruptive ages of only 0.2 Ma, indicate that they likely came from the same source caldera – either in the Stillwater Range or Clan Alpine Mountains (Figure 1; Brooks *et al.* 2008). Sierra Nevada ignimbrite 2 correlates with the TCC and with Tuff F of Brooks *et al.* (2008), and is sourced from a caldera in the Desatoya Mountains (Faulds *et al.* 2005; Figure 1). By integrating these geochemical and isotopic age correlations with palaeoaltimetry data from Cassel *et al.* (2009), we can quantify the change in elevation over the length of the palaeovalleys that Oligocene ignimbrites travelled in and characterize the Oligocene landscape morphology of what is now the Sierra Nevada – Basin and Range region.

Stable isotope palaeoaltimetry

Stable isotope palaeoaltimetry is based on the observation that the isotopic composition of precipitation changes with altitude due to Rayleigh distillation, resulting in progressive depletion of ^{18}O and D in meteoric water at higher elevations (Craig 1961; Dansgaard 1964; Ingraham and Taylor 1991; Chamberlain and Poage 2000; Rowley *et al.* 2001). Elevation acts as the dominant control on the hydrogen isotopic composition (δD) of precipitation, and δD scales at a predictable rate with change in elevation (Poage and Chamberlain 2001). Thus, the change in elevation along a transect can be estimated based on the change in δD of hydration water in volcanic glass. Post-eruption, meteoric water

enters glass in early low-temperature hydration and H^+ exchange for Na^+ and K^+ ions (Cerling *et al.* 1985). Within 5 ka of deposition, hydrated glass preserves the δD of ancient meteoric waters and does not exchange further once the glass is saturated (Friedman *et al.* 1993).

Cassel *et al.* (2009) used Oligocene volcanic glass samples from northern Sierra Nevada ignimbrites to estimate palaeoelevations. The δD of ancient hydration water in glass shard separates of 99% purity was determined at sample locations across the range, from deposits near palaeo-sea level at the edge of the Great Valley to samples in western Nevada. Sample values cannot be interpreted as a direct measure of δD of precipitation at the sample location, because higher elevation precipitation is incorporated into meteoric waters downstream through ground and surface transport. Glass thus records the δD of the hypsometric mean of the elevation of the drainage basin above that sample location (cf. Rowley *et al.* 2001; Rowley 2007). Lower in the basin, less-enriched precipitation is mixed with higher elevation, more-enriched meteoric waters, resulting in a smaller difference in meteoric water δD between low- and high-elevation samples than is present in precipitation δD, and an overall minimum estimate of topographic gradient (Rowley 2007). This estimate is nonetheless useful for discerning between tectonic models.

The δD of the volcanic glass samples from Cassel *et al.* (2009) decreases at a steady rate from -95 ± 3 and -115 ± 4‰ at the most westerly locations, to values ranging from -149 ± 7 to -156 ± 3‰ at the locations ~100 km east of the Ione marine deposits (Figure 5; all values relative to SMOW). This ~48‰ decrease in δD of meteoric water is similar to the isotopic gradient of precipitation over the range today (Ingraham and Taylor 1991), and reflects an increase in mean elevation from west to east at 31–28 Ma. Values from samples taken in western Nevada are between -145 and -160‰ δD, indicating no significant increase in Oligocene elevation farther east, consistent with either high topography with little change in elevation (high plateau), or lower elevations on the eastern side of a high range (rain shadow effect; see Poage and Chamberlain 2002). The spread in values probably indicates input in some sampled areas from another moisture source, as is common on modern plateau topography (Tian *et al.* 2007). These results show that the northern Sierra Nevada had a steep western gradient in the Oligocene, comparable with that of the modern range. Estimates of the Oligocene palaeoelevation of the northern Sierra Nevada, based on modern empirical and Oligocene modelled estimates of the isotopic lapse rate (the average change in δD with elevation), are 2800 ± 900 and $3200 + 1100/-2000$ m, respectively (Cassel *et al.* 2009). This study is consistent with the stable isotope palaeoaltimetry studies from the Eocene (Mulch *et al.* 2006) and Miocene (e.g. Chamberlain and Poage 2000; Crowley *et al.* 2008; Mulch *et al.* 2008), suggesting that the range was a significant topographic feature throughout the Cenozoic.

Discussion

The majority of ignimbrite samples from the northern Sierra Nevada can be correlated, based on their age and glass geochemistry, with one of three distinct ignimbrite units that have been mapped in western and central Nevada: the TAXC, TRC, and TCC (Henry *et al.* 2004; Faulds *et al.* 2005). These results show that ignimbrites 1 and 2 can be traced across the modern crest of the range into central Nevada, where source calderas are located (Henry 2008; Henry *et al.* 2004). The presence of correlative ignimbrites on either side of the modern crest of the Sierra Nevada shows that the Oligocene regional drainage divide was located to the east of its present position, at or east of the ignimbrite source calderas (Figure 1). These results also require that source calderas were located in a region of

similar or higher elevations than the drainages in which these ignimbrites were deposited, as ignimbrites can overtop at most ~600 m of topography (Fisher and Schmincke 1984).

Local east–west to northwest–southeast crustal extensions in the western Basin and Range also occurred in the Oligocene (Best and Christiansen 1991; Dilles and Gans 1995), although the timing of the onset of major faulting, and amount of total extension, varies widely across the province (Figure 4; Van Buer *et al.* 2009). Extension estimates across western and central Nevada are between 10 and 25% in western Nevada and 15 and 100% in central Nevada (Seedorf 1991; Smith *et al.* 1991; Surpless *et al.* 2002; Colgan *et al.* 2006; Van Buer *et al.* 2009). Using the maximum extension estimates for each region, we calculate that the TAXC, TRC, and TCC travelled at least 200 km from their source calderas (Figure 4). Based on the texture and lack of bedding, reworking, and sorting of ignimbrites throughout the Sierra Nevada, we estimate that ignimbrites were deposited up to 180 km from source calderas before their travel was significantly affected by fluvial transport (Figure 7).

Typically on low slopes, large-volume ignimbrites can travel 30–100 km from their source calderas (Watkins *et al.* 2002; Schmincke 2004), whereas large-volume ignimbrites flowing in steep Andean palaeovalleys off of the Peruvian Altiplano have been documented travelling upwards of 1000 km (Thouret *et al.* 2007). At the time of deposition, the Sierra Nevada is estimated to have reached elevations of 2700–3200 m (Cassel *et al.* 2009). This steep western slope in the Oligocene Sierra Nevada, and source calderas likely located in a region of high topography but relatively low relief to the east of the range, allowed for Oligocene ignimbrites to travel distances of 200 km or more.

The thickness of the sequence of ignimbrite deposits in Oligocene palaeovalleys gives a minimum estimate of the amount of valley relief, which ranges from over 700 m in western Nevada to 400 m near Haskell Peak in the high-elevation Sierra Nevada (Brooks *et al.* 2003; Faulds *et al.* 2005). Relief decreases drastically to 20 m or less in the lower elevations of the Sierra Nevada, where ignimbrites overlie wide fluvial braid plains of prevolcanic gravel. Generally, ignimbrite deposits gradually thin with distance from their source calderas, but the abrupt thinning of units at locations with underlying prevolcanic gravel probably reflects loss of confinement as the ignimbrites left bedrock-incised valleys and flowed out over the wide braid plains of the ancestral Yuba River.

Placed in the context of other recent studies (e.g. Wolfe *et al.* 1997; Mulch *et al.* 2006, 2008), the palaeoaltimetry and correlation data presented here for 31–28 Ma show that the range was likely a long-standing topographic feature throughout the Cenozoic, with a persistent steep western gradient and a region of high topography to the east of the range, where Oligocene source calderas were located. Little to no surface movement from the Oligocene to the present implies that uplift of the Sierra Nevada occurred in the Late Cretaceous to early Cenozoic, probably driven by geodynamic processes related to Mesozoic subduction along the Pacific margin, and coinciding with relatively faster exhumation rates (Cecil *et al.* 2006). Maximum late Cenozoic uplift in the northern Sierra Nevada, such as that proposed by Jones *et al.* (2004), is 700 m (present day lapse rate) or 1400 m (Oligocene modelled lapse rate; Cassel *et al.* 2009), although it is likely that mean surface elevations of the western flank of the range were not greatly affected by late Cenozoic tectonics (cf. Small and Anderson 1995; Wernicke *et al.* 1996; Cecil *et al.* 2006). These conclusions are also consistent with thermochronologic, palaeobotanical, and crustal structure studies throughout the Sierra Nevada–Basin and Range region, which also support Cenozoic high topography (Wernicke *et al.* 1996; Wolfe *et al.* 1997, 1998; House *et al.* 1997, 1998, 2001; Cecil *et al.* 2006; Colgan *et al.* 2006). After 28 Ma, westward-propagating extension, possibly related to the instability of the high topography (e.g. Coney and Harms

1984; Jones *et al.* 1998; Dilek and Moores 1999), lowered elevations to the east of the modern Sierra Nevada. The western side of the range maintained similar elevations from Miocene–Holocene (e.g. Crowley *et al.* 2008; Mulch *et al.* 2008), although extension affected the northernmost extent of the Sierra Nevada batholith (Van Buer *et al.* 2009).

Conclusions

We present new TREE geochemical data and $^{40}Ar/^{39}Ar$ radiometric ages of rhyolitic ignimbrite units exposed along the western slope and high peaks of the northern Sierra Nevada. TREE compositions in volcanic glass show three widespread, geochemically distinct, Sierra Nevada ignimbrite units that correlate to the TAXC, the TRC, and the TCC in western and central Nevada, identified and described by Henry *et al.* (2004) and Faulds *et al.* (2005). Single-crystal $^{40}Ar/^{39}Ar$ radiometric ages of sanidine and plagioclase from the Sierra Nevada ignimbrite units provide dates of 31.2, 30.9, and 28.7 Ma, which match the data from Nevada samples and therefore support this correlation. Using a palinspastic reconstruction of the Basin and Range extensional terrane, these results indicate that Oligocene ignimbrites travelled, at minimum, 200 km to the west from their source calderas. The Oligocene landscape, consisting of a region of high topography with a steep western slope, allowed for the distribution and long travel distance of ignimbrite units.

We hypothesize that these ignimbrites flowed downhill from a region of high topography that included what is now the Sierra Nevada and western–central Nevada (Nevadaplano), based on both ignimbrite correlation and palaeoelevation data from stable isotope compositions of hydrated volcanic glass from the Sierra Nevada ignimbrite units (Cassel *et al.* 2009). Palaeoaltimetry and thermochronology studies show that the range was likely a long-standing topographic feature throughout the Cenozoic (cf. House *et al.* 1998, 2001; Mulch *et al.* 2006, 2008), with a persistent steep western gradient and a region of high topography, where Oligocene source calderas were located (Figure 4). The high surface elevations present today cannot all be attributed to late Cenozoic tectonics; major surface uplift in the area of the northern Sierra Nevada occurred in the Late Cretaceous–early Cenozoic, probably driven by geodynamic processes related to Mesozoic subduction. This region of high topography was likely present from the late Eocene through the Oligocene and Miocene, and no drainage divide existed between the areas that are now the western flank of the Sierra Nevada and central Nevada. The modern crest of the Sierra Nevada formed in the late Miocene–Pliocene, as a result of Basin and Range extension lowering elevations to the east, with little to no associated northern Sierra Nevada surface uplift.

Acknowledgements

We thank Christopher Henry, who has shared his knowledge and expertise in western Nevada ignimbrite identification throughout our project, and Dean Miller and James Saburomaru at the US Geological Survey in Menlo Park for help with sample separation and irradiation preparations. Charles Knaack at Washington State University GeoAnalytical Lab performed the TREE geochemical analyses. Henry, Joseph Colgan and Bob Fleck provided constructive and insightful reviews. This research was supported by GSA and AAPG student grants and the Stanford University McGee Grant.

References

Ague, J.J., and Brimhall, G.H., 1988, Magmatic arc asymmetry and distribution of anomalous plutonic belts in the batholiths of California: Effects of assimilation, crustal thickness, and depth of crystallization: Geological Society of America Bulletin, v. 100, p. 912–927.

Bateman, P.C., and Wahrhaftig, C., 1966, Geology of the Sierra Nevada, *in* Bailey, E.H., ed., Geology of northern California: California division of mines and geology, Bulletin 190, p. 107–172.

Best, M.G., and Christiansen, E.H., 1991, Limited extension during peak Tertiary volcanism, Great Basin of Nevada and Utah: Journal of Geophysical Research, v. 96, no. B8, p. 13,509–13,528.
Best, M.G., Christiansen, E.H., Deino, A., Gromme, C.S., McKee, E.H., and Noble, D.C., 1989, Eocene through Miocene volcanism in the Great Basin of the Western United States: Bulletin – New Mexico Bureau of Geology and Mineral Resources, Report 131, 22 p.
Boyd, O.S., Jones, C.H., and Sheehan, A.F., 2004, Foundering lithosphere imaged beneath the southern Sierra Nevada, California, USA: Science, v. 305, p. 660–662.
Brooks, E.R., Wood, M.M., Boehme, D.R., Potter, K.L., and Marcus, B.I., 2003, Geologic map of the Haskell Peak area, Sierra County, California: California Geological Survey, Map Sheet 55, 1:12,000.
Brooks, E.R., Henry, C.D., and Faulds, J.E., 2008, Age and character of silicic ash-flow tuffs at Haskell Peak, Sierra County, California: Part of a major Eocene(?)–Oligocene paleovalleys spanning the Sierra Nevada-Basin and Range boundary: California Geological Survey, Map Sheet 55A, 39 p.
Cassel, E.J., Graham, S.A., and Chamberlain, P.C., 2009, Cenozoic tectonic and topographic evolution of the northern Sierra Nevada, California, through stable isotope paleoaltimetry: Geology, v. 37, p. 547–550.
Cecil, M.R., Ducea, M.N., Reiners, P.W., and Chase, C.G., 2006, Cenozoic exhumation of the northern Sierra Nevada, California, from (U–Th)/He thermochronology: Geological Society of America Bulletin, v. 118, no. 11/12, p. 1481–1488.
Cerling, T.E., Brown, F.H., and Bowman, J.R., 1985, Low-temperature alteration of volcanic glass: Hydration, Na, K, ^{18}O, and Ar mobility: Chemical Geology, v. 52, p. 281–293.
Chamberlain, C.P., and Poage, M.A., 2000, Reconstructing the paleotopography of mountain belts from the isotopic composition of authigenic minerals: Geology, v. 28, no. 2, p. 115–118.
Chen, J.H., and Moore, J.G., 1982, Uranium-lead isotopic ages from the Sierra Nevada batholith, California: Journal of Geophysical Research, v. 87, p. 4761–4784.
Colgan, J.P., Dumitru, T.A., Reiners, P.W., Wooden, J.L., and Miller, E.L., 2006, Cenozoic tectonic evolution of the Basin and Range Province in northwestern Nevada: American Journal of Science, v. 306, p. 616–654.
Coney, P.J., and Harms, T.A., 1984, Cordilleran metamorphic core complexes; Cenozoic extensional relics of Mesozoic compression: Geology, v. 12, p. 550–554.
Crafford, A.E.J., 2007, Geologic map of Nevada: USGS Data Series 249, 1 CD-ROM, 46 p., 1 plate.
Craig, H., 1961, Isotopic variations in meteoric waters: Science, v. 133, p. 1702–1703.
Crowley, B.E., Koch, P.L., and Davis, E.B., 2008, Stable isotope constraints on the elevation history of the Sierra Nevada Mountains, California: Geological Society of America Bulletin, v. 120, p. 588–598.
Dalrymple, G.B., 1964, Cenozoic chronology of the Sierra Nevada, California: University of California Publications in Geological Sciences, v. 47, 41 p.
Dansgaard, W., 1964, Stable isotopes in precipitation: Tellus 16, p. 436–468.
DeCelles, P.G., 2004, Late Jurassic to Eocene evolution of the Cordilleran thrust belt and foreland basin system, Western USA: American Journal of Science, v. 304, p. 105–168.
Deino, A.L., 1985, Stratigraphy, chemistry, K–Ar dating, and paleomagnetism of the Nine Hill Tuff, California-Nevada; Miocene/Oligocene ash-flow tuffs of Seven Lakes Mountain, California-Nevada; Improved calibration methods and error estimates for potassium-40-argon-40 dating of young rocks [Ph.D. thesis]: Berkeley, University of California, 457 p.
Deino, A.L., 1989, Single-crystal (super 40) Ar/(super 39) Ar dating as an aide in correlation of ash flows; examples from the Chimney Spring/New Pass tuffs and the Nine Hill/Bates Mountain tuffs of California and Nevada: Bulletin – New Mexico Bureau of Geology and Mineral Resources, Report 131, 70 p.
Dilek, Y., and Moores, E.M., 1999, A Tibetan model for the early Tertiary western United States: Journal of the Geological Society, London, v. 156, p. 929–941.
Dilles, J.H., and Gans, P.B., 1995, The chronology of Cenozoic volcanism and deformation in the Yerington area, western Basin and Range and Walker Lane: Geological Society of America Bulletin, v. 107, p. 474–486.
Ducea, M., 2001, The California arc: Thick granitic batholiths, eclogitic residues, lithospheric-scale thrusting and magmatic flare-ups: GSA Today, v. 11, no. 11, p. 4–10.

Ducea, M., and Saleeby, J., 1996, Buoyancy sources for a large, unrooted mountain range, the Sierra Nevada, California: Evidence from xenolith thermobarometry: Journal of Geophysical Research, v. 101, p. 8229–8244.

Ducea, M., and Saleeby, J., 1998, A case for delamination of the deep batholithic crust beneath the Sierra Nevada, California, *in* Ernst, W.G., and Nelson, C.A., eds., Integrated earth and environmental evolution of the southwestern United States: The Clarence A. Hall Jr. volume: Boulder, Colorado, Geological Society of America International Book Series ISB 001, p. 273–288.

Durrell, C., 1959, Tertiary stratigraphy of the Blairsden quadrangle, Plumas County, California: University of California Publications in Geological Sciences, v. 34, no. 3, p. 161–192.

England, P., and Molnar, P., 1990, Surface uplift, uplift of rocks, and exhumation of rocks: Geology, v. 18, p. 1173–1177.

Evernden, J.F., and James, G.T., 1964, Potassium-argon dates and the Tertiary floras of North America: American Journal of Science, v. 262, no. 8, p. 945–974.

Farley, K.A., 2002, (U–Th)/He dating: Techniques, calibrations, and applications: Reviews in Mineralogy and Geochemistry, v. 47, p. 819–844.

Faulds, J.E., Henry, C.D., and Hinz, N.H., 2005, Kinematics of the northern Walker Lane: An incipient transform fault along the Pacific–North American plate boundary: Geology, v. 33, p. 505–508.

Friedman, I., Gleason, J., and Warden, A., 1993, Ancient climate from deuterium content of water in volcanic glass, *in* Swart, P.K., Lohmann, K.C., McKenzie, J., and Savin, S., eds., Climate change in continental isotopic records: Geophysical monograph 78, American Geophysical Union, p. 309–319.

Fisher, R.V., and Schmincke, H.U., 1984, Pyroclastic rocks: Berlin, Springer-Verlag, 472 p.

Garside, L.J., Castor, S.B., dePolo, C.M., and Davis, D.A., 2003, Geologic map of the Fraser Flat Quadrangle and the west half of the Moses Rock Quadrangle, Washoe County, Nevada: 1:24,000, Nevada Breau of Mines and Geology, Map 146.

Garside, L.J., Henry, C.D., Faulds, J.E., and Hinz, N.H., 2005, The upper reaches of the Sierra Nevada auriferous gold channels, California and Nevada, *in* Rhoden, H.N., Steininger, R.C., and Vikre, P.G., eds., Geological Society of Nevada Symposium 2005: Window to the World, May 2005, Nevada: Reno, p. 209–235.

Girty, G.H., Hanson, R.E., Schweickert, R.A., Harwood, D.S., eds., 1996, The Northern Sierra terrane and associated mesozoic magmatic units: Implications foe the tectonic history of the western Cordillera: Pacific Section SEPM, Book 81, 92 p.

Gregory-Wodzicki, K.M., 1997, The late Eocene House Range flora, Sevier Desert, Utah; paleoclimate and paleoelevation: Palaios, v. 12, p. 552–567.

Henry, C.D., 2008, Ash-flow tuffs and paleovalleys in northeastern Nevada; implications for Eocene paleogeography and extension in the Sevier hinterland, northern Great Basin: Geosphere, v. 4, no. 1, p. 1–35.

Henry, C.D., Faulds, J.E., dePolo, C.M., and Davis, D.A., 2004, Geologic map of the Dogskin mountain quadrangle, Washoe County, Nevada: Nevada Bureau of Mines and Geology Map 148, 1:24,000.

Hildreth, W., and Mahood, G., 1985, Correlation of ash-flow tuffs: Geological Society of America Bulletin, v. 96, no. 7, p. 968–974.

Horton, T.W., Sjostrom, D.J., Abruzzese, M.J., Poage, M.A., Waldbauer, J.R., Hren, M., Wooden, J., and Chamberlain, C.P., 2004, Spatial and temporal variation of Cenozoic surface elevation in the Great Basin and Sierra Nevada: American Journal of Science, v. 304, p. 862–888.

House, M.A., Wernicke, B.P., Farley, K.A., and Dumitru, T.A., 1997, Cenozoic thermal evolution of the central Sierra Nevada, California, from (U–Th)/He thermochronometry: Earth and Planetary Science Letters, v. 151, p. 167–179.

House, M.A., Wernicke, B.P., and Farley, K.A., 1998, Dating topography of the Sierra Nevada, California, using apatite (U–Th)/He ages: Nature, v. 396, p. 66–69.

House, M.A., Wernicke, B.P., and Farley, K.A., 2001, Paleo-geomorphology of the Sierra Nevada, California, from (U–Th)/He ages in apatite: American Journal of Science, v. 301, p. 77–102.

Huber, N.K., 1981, Amount and timing of late Cenozoic uplift and tilt of the central Sierra Nevada, California – Evidence from the upper San Joaquin river basin: US Geological Survey Professional Paper, no. 1197, 28 p.

Huber, N.K., 1990, The late Cenozoic evolution of the Tuolumne River, central Sierra Nevada, California: Geological Society of America Bulletin, v. 102, p. 102–115.
Hudson, F.S., 1960, Post-Pliocene uplift of the Sierra Nevada, California: Geological Society of America Bulletin, v. 71, p. 1547–1574.
Ingraham, N.L., and Taylor, B.E., 1991, Light stable isotope systematics of large-scale hydrologic regimes in California and Nevada: Water Resources Research, v. 27, p. 77–90.
John, D.A., 1995, Tilted middle Tertiary ash-flow calderas and subjacent granitic plutons, southern Stillwater Range, Nevada: Cross sections of an Oligocene igneous center: Geological Society of America Bulletin, v. 107, p. 180–200.
John, D.A., Henry, C.D., and Colgan, J.P., 2008, Magmatic and tectonic evolution of the Caetano caldera, north-central Nevada: A tilted, mid-Tertiary eruptive center and source of the Caetano Tuff: Geosphere, v. 4, no. 1, p. 75–106.
Jones, C.H., Farmer, G.L., and Unruh, J., 2004, Tectonics of Pliocene removal of lithosphere of the Sierra Nevada, California: Geological Society of America Bulletin, v. 116, no. 11/12, p. 1408–1422.
Jones, C.H., Sonder, L.J., and Unruh, J.R., 1998, Lithospheric gravitational potential energy and past orogenesis: Implications for conditions of initial Basin and Range and Laramide deformation: Geology, v. 26, p. 639–642.
Lindgren, W., 1911, The Tertiary gravels of the Sierra Nevada of California: US Geological Survey Professional Paper 73, 226 p.
MacGinitie, H.D., 1941, A middle Eocene flora from the central Sierra Nevada: Carnegie Institution of Washington Publication, 178 p.
Molnar, P., and Chen, W.P., 1983, Focal depths and fault plane solutions of earthquakes under the Tibetan Plateau: Journal of Geophysical Research, v. 88 no. B2, p. 1180–1196.
Mulch, A., Graham, S.A., and Chamberlain, C.P., 2006, Hydrogen isotopes in Eocene river gravels and paleoelevation of the Sierra Nevada: Science, v. 313, p. 87–89.
Mulch, A., Sarna-Wojcicki, A.M., Perkins, M.E., and Chamberlain, C.P., 2008, A Miocene to Pleistocene climate and elevation record of the Sierra Nevada (California): Proceedings of the National Academic Sciences, v. 105, p. 6819–6824.
Poage, M.A., and Chamberlain, C.P., 2001, Empirical relationships between elevation and the stable isotope composition of precipitation and surface waters: Considerations for studies of paleoelevation change: American Journal of Science, v. 301, p. 1–15.
Poage, M.A., and Chamberlain, C.P., 2002, Stable isotopic evidence for a pre-Middle Miocene rain shadow in the western Basin and Range: Implications for the paleotopography of the Sierra Nevada: Tectonics, v. 21, no. 4, p. 1–9.
Rowley, D.B., 2007, Stable isotope-based paleoaltimetry: Theory and validation: Reviews in Mineralogy and Geochemistry, v. 66, p. 23–52.
Rowley, D.B., Pierrehumbert, R.T., and Currie, B.S., 2001, A new approach to stable isotope-based paleoaltimetry: Implications for paleoaltimetry and paleohypsometry of the High Himalaya since the Late Miocene: Earth and Planetary Science Letters, v. 188, p. 253–268.
Saucedo, G.J., and Wagner, D.L., 1992, Map of the Chico Quadrangle, California, 1:250,000: Regional Geologic Map Series, California Division of Mines and Geology.
Saucedo, G.J., Fulford, M.M., Mata-Sol, R.A., and Lindquist, T.A., 1992, Radiometric ages of rocks in the Chico quadrangle, California: California Division of Mines and Geology Regional Geologic Map Series Map No. 7A, Sheet 4, 21 p.
Schmincke, H., 2004, Volcanism: Berlin: Springer-Verlag, 324 p.
Seedorf, E., 1991, Magmatism, extension and ore deposits of Eocene to Holocene age in the Great Basin–Mutual effects and preliminary proposed genetic relationships, *in* Raines, G.L., and Wilkinson, W.H., eds., Geology and ore deposits of the Great Basin: Reno, Geological Society of Nevada, p. 133–178.
Small, E.E., and Anderson, R.S., 1995, Geomorphically driven late Cenozoic rock uplift in the Sierra Nevada, California: Science, v. 270, p. 277–280.
Smith, D.L., Gans, P.B., and Miller, E.L., 1991, Palinspastic restoration of Cenozoic extension in the central and eastern Basin and Range Province at latitude 39–40 degrees N, *in* Raines, G.L., Lisle, R.E., Schafer, R.W., and Wilkinson, W.H., eds., Geology and ore deposits of the Great Basin; Symposium Proceedings, p. 75–86.
Sonder, L.J., and Jones, C.H., 1999, Western United States extension; how the west was widened: Annual Review of Earth and Planetary Sciences, v. 27, p. 417–462.

Sonder, L.J., England, P.C., Wernicke, B.P., and Christiansen, R.L., 1987, A physical model for Cenozoic extension of western North America, *in* Coward, M.P., Dewey, J.F., and Hancock, P.L., eds., Continental extensional tectonics: Geological Society Special Publications, v. 28, p. 187–201.

Sun, S.S., and McDonough, W.F., 1989, Chemical and isotopic systematics of oceanic basalts; implications for mantle composition and processes: Geological Society Special Publications, v. 42, p. 313–345.

Surpless, B.E., Stockli, D.F., Dumitru, T.A., and Miller, E.L., 2002, Two-phase westward encroachment of Basin and Range extension into the northern Sierra Nevada: Tectonics, v. 21, p. 1–13.

Tian, L., Yao, T., MacClune, K., White, J.W.C., Schilla, A., Vaughn, B., Vachon, R., and Ichiyanagi, K., 2007, Stable isotopic variations in west China: A consideration of moisture sources: Journal of Geophysical Research, v. 112, D10112, 12 p.

Thouret, J.-C., Wörner, G., Gunnell, Y., Singer, B., Zhang, X., and Souriot, T., 2007, Geochronologic and stratigraphic constraints on canyon incision and Miocene uplift of the Central Andes in Peru: Earth and Planetary Science Letters, v. 263, p. 151–166.

Unruh, J.R., 1991, The uplift of the Sierra Nevada and implications for late Cenozoic epeirogeny in the western Cordillera: Geological Society of America Bulletin, v. 103, p. 1395–1404.

Van Buer, N.J., Miller, E.L., and Dumitru, T.A., 2009, Early Tertiary paleogeologic map of the northern Sierra Nevada Batholith and the northwestern Basin and Range: Geology, v. 37, p. 371–374.

Wagner, D.L., Saucedo, G.J., and Grose, T.L.T., 2000, Tertiary volcanic rocks of the Blairsden area, northern Sierra Nevada, California, *in* Brooks, E.R., and Dida, L.T., eds., Field guide to the geology and tectonics of the northern Sierra Nevada: State of California, Department of Conservation, Division of Mines and Geology, Sacramento, CA, United States (USA), Report 122, p. 155–172.

Wakabayashi, J., and Sawyer, T.L., 2001, Stream incision, tectonics, uplift and evolution of topography of the Sierra Nevada, California: The Journal of Geology, v. 109, p. 539–562.

Watkins, S.D., Giordano, G., Cas, R.A.F., and De Rita, D., 2002, Emplacement processes of the mafic Villa Senni Eruption Unit (VSEU) ignimbrite succession, Colli Albani volcano, Italy: Journal of Volcanology and Geothermal Research, v. 118, p. 173–203.

Wernicke, B., Clayton, R., Ducea, M., Jones, C.H., Park, S., Ruppert, S., Saleeby, J., Snow, J.K., Squires, L., Fliedner, M., Jiracek, G., Keller, R., Klemperer, S., Luetgert, J., Malin, P., Miller, K., Mooney, W., Oliver, H., and Phinney, R., 1996, Origin of high mountains in the continents: The southern Sierra Nevada: Science, v. 271, p. 190–193.

Whipple, K.X., Kirby, E., and Brocklehurst, S.H., 1999, Geomorphic limits to climate-induced increases in topographic relief: Nature, v. 401, p. 39–43.

Wolfe, J.A., 1992, Climatic, floristic, and vegetational changes near the Eocene/Oligocene boundary in North America, *in* Prothero, D.R., and Berggren, W.A., eds., Eocene–Oligocene climatic and biotic evolution: Princeton, NJ: Princeton University Press, p. 421–436.

Wolfe, J.A., Schorn, H.E., Forest, C.E., and Molnar, P., 1997, Paleobotanical evidence for high altitudes in Nevada during the Miocene: Science, v. 276, p. 1672–1675.

Wolfe, J.A., Forest, C.E., and Molnar, P., 1998, Paleobotanical evidence of Eocene and Oligocene paleoaltitudes in midlatitude North America: Geological Society of America Bulletin, v. 110, p. 664–678.

Yeend, W.E., 1974, Gold-bearing gravel of the ancestral Yuba River, Sierra Nevada, California: US Geological Survey Professional Paper 772, 44 p.

Zandt, G., Gilbert, H., Owens, T.J., Ducea, M., Saleeby, J., and Jones, C.H., 2004, Active foundering of a continental arc root beneath the southern Sierra Nevada in California: Nature, v. 431, p. 41–46.

Supplementary Material Online

Detailed description (1) of $^{40}Ar/^{39}Ar$ geochronology and TREE geochemistry analytical techniques, (2) a table of each individual age determination, (3) a K/Ca Discrimination plot for samples with ages between 31.0 and 31.2 Ma, and (4) a table of TREE concentrations on matrix volcanic glasses (all values in ppm).